Accumulation of unstable periodic orbits and the stickiness in the two-dimensional piecewise linear map

A. Akaishi* and A. Shudo
Department of Physics, Tokyo Metropolitan University, Minami-Osawa, Hachioji, Tokyo 192-0397, Japan
(Received 2 September 2009; published 23 December 2009)

We investigate the stickiness of the two-dimensional piecewise linear map with a family of marginal unstable periodic orbits (FMUPOs), and show that a series of unstable periodic orbits accumulating to FMUPOs plays a significant role to give rise to the power law correlation of trajectories. We can explicitly specify the sticky zone in which unstable periodic orbits whose stability increases algebraically exist, and find that there exists a hierarchy in accumulating periodic orbits. In particular, the periodic orbits with linearly increasing stability play the role of fundamental cycles as in the hyperbolic systems, which allows us to apply the method of cycle expansion. We also study the recurrence time distribution, especially discussing the position and size of the recurrence region. Following the definition adopted in one-dimensional maps, we show that the recurrence time distribution has an exponential part in the short time regime and an asymptotic power law part. The analysis on the crossover time T_c^* between these two regimes implies $T_c^* \sim -\log[\mu(R)]$ where $\mu(R)$ denotes the area of the recurrence region.

DOI: 10.1103/PhysRevE.80.066211 PACS number(s): 05.45.−a

I. INTRODUCTION

The slow dynamics in Hamiltonian systems has been investigated in the past few decades and is still under discussion to make their mechanism and quantitative estimation clear [1–14]. Phase space of Hamiltonian systems is so complex in general; besides chaotic components, a variety of invariant components such as Kolmogorov-Arnold-Moser (KAM) tori, islands of stability, or cantori coexist in a single phase space. Difficulties lie in such immense complexity of phase space and inhomogeneity originating from various invariant structures. Chaotic trajectories exhibit regular motions in the neighborhood of invariant tori where they spend a very long time, while they behave quite irregularly far apart from invariant tori or islands of stability. This slow motion, so-called stickiness, leads asymptotic power law decay in statistical quantities.

One of the most reliable tools to examine the stickiness numerically is the distribution of the recurrence time defined as

$$P_R(T) = \mu[\{x \in R | \tau_R(x) = T\}]/\mu(R), \tag{1}$$

where μ is the invariant measure, and R a compact region in phase space called the recurrence region. $\tau_R(x)$ is the first recurrence time from an initial point x to the recurrence region R. Chirikov and Shepelyansky have studied the cumulative distribution of $P_R(T)$,

$$Q_R(T) = \sum_{T'=T}^{\infty} P_R(T'), \tag{2}$$

and proposed that the power law exponent has a universality property [15,16]. Several related works follow thereafter, some assert universality and others not [9,10,17,18].

The situation becomes simple if one considers the system with sharply divided phase space, and exactly for this reason recent analyses could reveal more clearly how sticky motions along the boundaries occur and under what mechanism the recurrence time distribution exhibits power law tails [19,20]. In a class of the mushroom billiards where a regular component and chaotic components coexist with sharp boundaries, a direct analysis of injection and escape regions for the hat region of mushroom predicts explicitly the power law exponent [21]. In the case of stadium billiards, it was shown that the survival probability and the recurrence time distribution obeys the power law with an integer-valued exponent because of the existence of a family of marginally unstable periodic orbits (FMUPOs) which form a line-shaped structure in phase space [22].

However, even in such simple situations, the arguments need several assumptions. Even though there is no doubt that sticky boundaries control the slow motion, detailed mechanisms have not been understood yet, for example, as to whether or not the sticky zone can be explicitly specified, which types of orbits coexist in the sticky zone, or what are the most relevant ones among the sticky orbits.

One should also note that even in the definition of statistical measure some ambiguities remain as compared to the arguments for one-dimensional systems [23–25]. As discussed below, the position or size of the recurrence region R has not seriously been discussed in two-dimensional cases, whereas it was pointed out that subtleness exists in one-dimensional maps [24].

The first part of the present paper is devoted to investigating the structure of periodic orbits for a two-dimensional piecewise linear map with FMUPOs to elucidate more explicit mechanism causing the sticky motion. We show that there exist periodic orbits accumulating to FMUPOs, and the power law behavior certainly originates from them. We can specify the region in which accumulating periodic orbits exist. This allows us to investigate the survival probability, which is a simpler measure than the recurrence time distri-

*akaisi-akira@ed.tmu.ac.jp

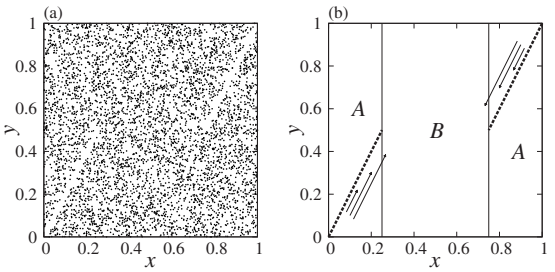

FIG. 1. (a) A phase space portrait with $K=4$. (b) FMUPOs are shown by broken lines in the region A of phase space. The arrows parallel to FMUPOs schematically represent the motion along FMUPOs and their length is proportional to a distance to FMUPOs.

bution. In particular, the analysis of the periodic orbit expansion reveals that the periodic orbits whose stabilities increase linearly with their period play the role of *fundamental cycle*, as in the so-called cycle expansion for uniformly hyperbolic systems, and cancel the contribution from periodic orbits with polynomial increase in the stabilities. We show that the most relevant periodic orbits thus picked up are responsible for the power law decay observed in the survival probability.

The second part of the present paper concerns the definition of the recurrence time distribution. In numerical calculations, we usually take a recurrence region R with a finite size, $\mathrm{Area}(R)>0$, and observes the power law decay. However, if we define the recurrence time distribution in the limit of $\mathrm{Area}(R)\to 0$, as done in Ref. [23], we find an exponential function, thereby the power law decay should be regarded as a finite size effect. More precisely, after making a proper normalization for the recurrence time, we show that there exists a crossover time scale T_c^* at which the exponential decay switches to the power law tail [11,12,26,27], and T_c^* tends to infinity as the size of the recurrence region $\mathrm{Area}(R)$ shrinks to zero.

II. PIECEWISE LINEAR MAPS

Let us consider the two-dimensional area-preserving map on torus $\mathbf{T}^2:=[0,1)\times[0,1)$ defined as

$$x' \equiv x + y' \mod 1,$$

$$y' \equiv y + Kf(x) \mod 1, \tag{3}$$

where K is a positive parameter and $f(x)$ is a piecewise linear function given as

$$f(x) = \begin{cases} -x & \text{if } x \in \left[0,\frac{1}{4}\right), \\ -1/2 + x & \text{if } x \in \left[\frac{1}{4},\frac{3}{4}\right), \\ 1-x & \text{if } x \in \left[\frac{3}{4},1\right). \end{cases} \tag{4}$$

Let A denote the region of phase space $([0,\frac{1}{4})\cup[\frac{3}{4},1))\times[0,1)$ and B denote the region $[\frac{1}{4},\frac{3}{4})\times[0,1)$ [see Fig. 1(b)]. Note that the stability matrix in A is elliptic for $0<K<4$, parabolic for $K=4$ and hyperbolic for $K>4$. The stability matrix in B is hyperbolic for $K>0$. For the map with $0<K<4$, the stable islands and the chaotic components coexist in phase space. For $K\geq 4$ it was rigorously proved that the map is fully chaotic and no stable islands exist in phase space [28].

A. Map with $K=4$

For $K=4$, the map is rewritten as

$$\begin{pmatrix} x' \\ y' \end{pmatrix} \equiv \begin{cases} M_A \begin{pmatrix} x \\ y \end{pmatrix} & \mod 1 \quad \text{if } (x,y) \in A, \\ M_B \begin{pmatrix} x \\ y \end{pmatrix} & \mod 1 \quad \text{if } (x,y) \in B, \end{cases} \tag{5}$$

where

$$M_A = \begin{pmatrix} -3 & 1 \\ -4 & 1 \end{pmatrix}, \quad M_B = \begin{pmatrix} 5 & 1 \\ 4 & 1 \end{pmatrix}. \tag{6}$$

The stable islands which exist for $0<K<4$ shrink to form FMUPOs. Phase space portrait for $K=4$ is shown in Fig. 1(a). FMUPOs are a one-parameter family of unstable periodic orbits with null stability exponent and has zero measure in phase space. The simplest scenario of the stickiness is based on the slow motion along FMUPOs, as studied in stadium or mushroom billiards [20–22].

In the region B, the orbits are hyperbolic, and the motion in A is a constant shift parallel to the direction of FMUPOs and the amount of the shift is proportional to the distance from FMUPOs since M_A is parabolic. FMUPOs consist of periodic orbits with period 2, and each periodic point is aligned symmetrically with respect to the center of the phase space [see Fig. 1(b)]. The direction of FMUPOs is parallel to the direction of the eigenvector of M_A.

B. Periodic orbits of the piecewise linear map

Since the map we consider is piecewise linear, enumerating periodic orbits is straightforward. A concrete procedure is presented in Appendix A. We assign either symbol A or B to a given orbit according to which region the orbit visits at each step. Then each periodic orbit of the map is expressed as a finite sequence of the symbols A and B. Note that the number of periodic orbits for a given finite sequence is not necessarily one since the partition into A and B is not generating.

In Fig. 2(a) we plot all the unstable periodic orbits whose period is less than 6 for the map with $K=4$. Clearly, the periodic points are not uniformly distributed in phase space. In particular, the periodic points around FMUPOs are sparse. This is because the periodic orbits lying in such sparse regions have quite long periods. It is also easy to see that the stability exponent of the periodic orbits close to FMUPOs is rather small compared to the others. The distributions of the stability exponents of unstable periodic orbits are shown in Fig. 2(b). We notice that there exist unstable periodic orbits with small stability exponents, for example, in case of period 7 and period 9.

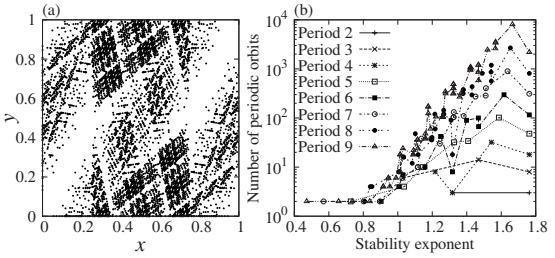

FIG. 2. (a) The periodic points of all unstable periodic orbits whose period is less than 6 for the map with $K=4$. (b) The distributions of the stability exponents of the unstable periodic orbits.

In Appendix B we prove there exists a series of unstable periodic orbits whose stability increases polynomially as a function of their period. As shown in Appendix B, the symbolic sequences of these orbits are expressed as combinations of $A^{\ell}B$ and $A^{m}B^{2}$ where ℓ and m are integers. Suppose that the block $A^{\ell}B$ appears p times and $A^{m}B^{2}$ q times in a periodic orbit with length t. Let $\ell_1,\ldots,\ell_p$ be the number of A in the block $A^{\ell}B$, and similarly, $m_1,\ldots,m_q$ be the number of A in the type $A^{m}B^{2}$. Since M_A is a parabolic matrix, each matrix element in $M_A^{\ell}M_B$ ($M_A^{m}M_B^{2}$) is proportional to ℓ (m), the eigenvalues of the stability matrices of such a periodic orbit are approximately $\ell_1\cdots\ell_p m_1\cdots m_q$ while the period t is given as $t\sim\ell_1+\cdots+\ell_p+m_1+\cdots+m_q$. Therefore, the stability exponent grows as $\log(t^{p+q})/t$ for large t. This implies the existence of infinitely many periodic orbits whose stability exponents are smaller than an arbitrary small value.

Such a set of periodic orbits is also found in phase space with the sharp boundaries between stable islands and chaotic sea. For $K_n=2(1+\cos\frac{\pi}{n})$ $(n=2,3,\ldots)$, it was shown that there appears a single stable island of a $2n$-sided polygon with a surrounding chaotic component [28]. The stable island is composed of periodic orbits of period n. Two edges of the stable polygon lie on the border between A and B. The coordinates of end points of the edge are, respectively, given as $(1/4,1/2)$ and $(1/4,(K_n-2)/4)$. On the edges of the polygon, orbits have the marginal stability since the stability matrix of orbits of $A^{n-1}B$ becomes parabolic. In the B region close to the edges, the motion of orbits is a constant shift parallel to the edge. Then one can provide, similarly in Appendix B, a systematic procedure to find periodic orbits accumulating to the edges (see Ref. [29]). A slight difference is as follows: in case of $K=4$, A represents the linear shift and B the hyperbolic transformation, while in $K_n=2(1+\cos\frac{\pi}{n})$ $(n=2,3,\ldots)$ case, the symbol $A^{n-1}B$ represents a constant shift and $A^{n-2}B$ a hyperbolic transformation in the region close to the polygon. In Fig. 3, we show periodic orbits for $K=2(n=2)$ and $K=3(n=3)$, in which only periodic orbits of the type $(A^{n-1}B)^{\ell}A^{n-2}B$ are depicted.

The existence of the periodic orbits accumulating to the boundary of stable islands is pointed out in the study for $K=1$ and for the stadium billiards [6,30]. Here, we have obtained a wider class of the accumulating periodic orbits, which is the series of periodic orbits whose stability increases as a polynomial function of its period.

III. PERIODIC ORBIT EXPANSIONS

The asymptotic power law, observed in the survival probability or the decay of correlations, is a characteristic phenomenon in nonhyperbolic systems. In this section, we will show that periodic orbits accumulating to FMUPOs are certainly responsible for the power law decay of the survival probability.

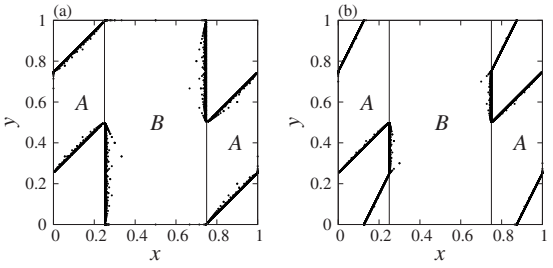

FIG. 3. Unstable periodic orbits accumulating to the boundary of a stable island. (a) Phase space for $K=2$. (b) $K=3$. The periodic orbits are represented as $(A^{n-1}B)^{\ell}A^{n-2}B$. In (a) and (b), periodic points for $\ell=1,\ldots,20$ are plotted.

The asymptotic behavior of dynamical quantities is related to the spectra of the Perron-Frobenius operator $\mathcal{L}$, which describes a unit time evolution of the density distribution [31]. The spectral properties of $\mathcal{L}$ are investigated through the determinant $\det(1-z\mathcal{L})$. If the system is uniformly hyperbolic, the determinant is represented, using periodic orbit expansions [31,32], as

$$\det(1-z\mathcal{L})=\prod_{s=0}^{\infty}\prod_{p\in\mathcal{P}_{\rm all}}\left(1-\frac{z^{t_p}}{|\Lambda_p|\Lambda_p^{s}}\right), \tag{7}$$

where $\mathcal{P}_{\rm all}$ denotes all prime periodic orbits and t_p and Λ_p period and linear stability of the periodic orbit p, respectively.

Since we hereafter focus on the survival probability, instead of the determinant (7), we consider the dynamical zeta function with respect to the chaotic component. The inverse of the zeta function is given as

$$\frac{1}{\zeta(z)}=\prod_{p\in\mathcal{P}}\left(1-\frac{z^{t_p}}{|\Lambda_p|}\right), \tag{8}$$

where $\mathcal{P}$ denotes all unstable periodic orbits of prime cycle in the chaotic component.

We now develop our arguments following that for one-dimensional intermittent maps. Recall that for one-dimensional intermittent maps the product over prime periodic orbits after excluding marginal fixed points describes the intermittent part of dynamics [25,32]. In analogy with the intermittent maps, we discuss the asymptotic power law of the present map by investigating the periodic orbit expansion of the zeta function (8).

The simplest situation exhibiting the power law would be $K=4$ in our map. So, we restrict ourselves to the $K=4$ case, in which phase space contains FMUPOs, but their measure is zero. This allows us to consider the product of the periodic orbit expansion which runs over all periodic orbits except for FMUPOs.

In order to see the survival probability, we slightly modify our map [Eq. (5)] so as to have a leaking region, and regard the orbits reaching the leaking region as escaped from the

system. A similar treatment with such leaking regions was recently made in Refs. [11,12]. We define the survival probability $S_L(n)$ for the system with the leaking region L by

$$S_L(n) = \mu(\{x \in X \setminus L\} | \tau'_L(x) = n)/\mu(X \setminus L), \tag{9}$$

where X and $\tau'_L(x)$ denote the phase space and the first hitting time from a point x to the region L, respectively. An asymptotic decay of $S_L(n)$ is evaluated by the linear stability of periodic orbits,

$$S_L(n) \sim \Gamma_n = \sum_p^{(n)} \frac{1}{|\Lambda_p|}, \tag{10}$$

where the sum $\Sigma_p^{(n)}$ runs over the periodic orbits with period n which lie outside the leaking region L. The survival probability is then linked to the dynamical zeta function by the formula

$$\Gamma_n = \frac{1}{2\pi i} \oint_{\gamma_r} z^{-n} \left(\frac{d}{dz} \log \zeta^{-1}(z) \right) dz, \tag{11}$$

where γ_r denotes a contour that encircles the origin in the clockwise direction inside the unit circle [32]. The asymptotic behavior of Γ_n can be discussed through the analytic property of $1/\zeta$ in the complex plane.

The inverse zeta function $1/\zeta$ is expressed by the product over periodic orbits (8), and expanded with coefficients c_n as

$$\prod_{p \in \mathcal{P}} \left(1 - \frac{z^{t_p}}{|\Lambda_p|} \right) = 1 - \sum_{n=1}^{\infty} c_n z^n. \tag{12}$$

Below we will show that the zeta function in the asymptotic regime is controlled by a subset of periodic orbits accumulating to FMUPOs, not necessarily all the unstable periodic orbits $\mathcal{P}$.

To this end, we first show that the periodic orbits accumulating to FMUPOs cause the power law decay in the survival probability. Let $\mathcal{A}$ be a set of periodic orbits whose stability increases algebraically in their length. As mentioned in Sec. II B, such periodic orbits are expressed as combinations of $A^\ell B$ and $A^m B^2$ (see also Appendix B). Note that periodic points in $\mathcal{A}$ are distributed in a restricted region around FMUPOs as shown in Fig. 4. Then we consider the product over $\mathcal{A}$ and its expansion with coefficients a_n

$$\prod_{p \in \mathcal{A}} \left(1 - \frac{z^{t_p}}{|\Lambda_p|} \right) = 1 - \sum_{n=1}^{\infty} a_n z^n. \tag{13}$$

Since the orbits around FMUPOs are sticky and the set of periodic orbits $\mathcal{A}$ is associated with these sticky orbits, it is natural to expect that the $\mathcal{A}$ controls the power law behavior. This can actually be verified by comparing the behavior of the coefficients c_n with those of a_n in the large n regime. As shown in Fig. 5(a), the coefficients a_n well reproduce an expected n dependence, that is $a_n \sim 1/n$. (As shown in the next subsection, $1/n$ yields the power law in the survival probability.) As also noticed in Fig. 5(b), the difference $|c_n - a_n|$ decreases exponentially with n. Therefore we may attribute the power law behavior to the set of periodic orbits accumulating to FMUPOs.

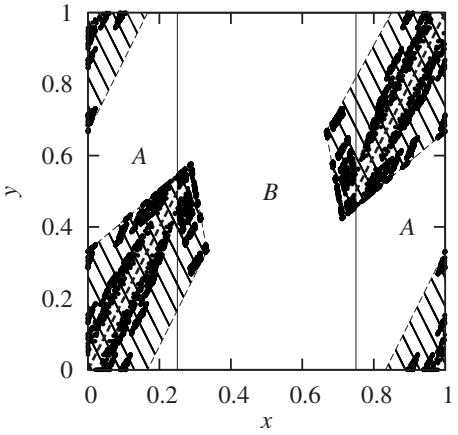

FIG. 4. The periodic points of periodic orbits in $\mathcal{A}$. The periodic orbits whose period is less than 15 are shown. They are located in a restricted region around FMUPOs. Here FMUPOs are shown by the broken lines. The shaded region shows the bounding area in which the periodic points lie. The vertex coordinates of the shaded polygon are (1/3,1/3), $(\sqrt{3}/6, \sqrt{3}/3)$, (0,1/3), (2/3,2/3), $(1-\sqrt{3}/6, 1-\sqrt{3}/3)$, and (1,2/3).

Although there is no rigorous proof for the behavior numerically observed, the result itself is a reasonable one. However, this is not the end of the story. Due to the simplicity of the system, we can specify more explicitly the origin of power law decay by examining the structure of $\mathcal{A}$ closely.

In order to explain such a structure in $\mathcal{A}$, let $\mathcal{F}^{(1)}$ denote a set of periodic orbits whose symbolic representations are given as $\{A^{2k}B\}_{k\geq 1}$ and $\{A^{2k-1}B^2\}_{k\geq 1}$. As mentioned in the previous section, one can show that $\mathcal{F}^{(1)}$ consists of periodic orbits whose stability increases *linearly*. Note that the period of periodic orbits in $\mathcal{F}^{(1)}$ is odd. We next define $\mathcal{F}^{(2)}$ as the set of periodic orbits in such a way that the symbolic representations are given as

$$\{A^{2k_1-1}BA^{2k_2-1}B\}_{k_1\geq 1, k_2 \geq 1},$$

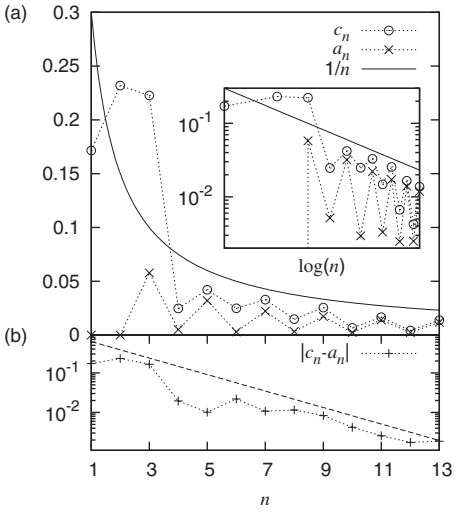

FIG. 5. (a) The expansion coefficient c_n (circles) and a_n (crosses). Inset: the same plot in logarithmic scale. The solid line represents $1/n$, which is a guide to the eyes. (b) The difference $|c_n - a_n|$. The broken line is an exponential curve fitted to $|c_n - a_n|$ in the large n region.

$$\{A^{2k_1-1}BA^{2k_2}B^2\}_{k_1\geq 1,k_2\geq 1},$$

$$\{A^{2k_1}B^2A^{2k_2}B^2\}_{k_1\geq 1,k_2\geq 1}. \tag{14}$$

The period of periodic orbits in $\mathcal{F}^{(2)}$ is even and the stability increases quadratically as k_1 and k_2 increase.

Now we discuss the role of the union of $\mathcal{F}^{(1)}$ and $\mathcal{F}^{(2)}$, that is, $\mathcal{F}=\mathcal{F}^{(1)}\cup\mathcal{F}^{(2)}$. Suppose an arbitrary periodic orbit in the set $\mathcal{A}\backslash\mathcal{F}$ with the corresponding symbolic representation, say $A^{2\ell_1}BA^{2\ell_2}B$. Then we can show that there exist periodic orbits in $\mathcal{F}^{(1)}$ whose symbolic representation is, respectively, given as $A^{2\ell_1}B$ and $A^{2\ell_2}B$.

In the same way, any periodic orbit in $\mathcal{A}\backslash\mathcal{F}$ can be decomposed into those orbits which are contained in $\mathcal{F}$. This is justified as follows: let us consider a symbol sequence in which the blocks $A^\ell B$ and A^mB^2 appear p and q times, respectively. We denote the total length of the sequence by t. Suppose that $(p+q)+t$ is an even number. If $(p+q)$ and t are both odd numbers, the sequence must contain, at least, a symbol sequence of $A^{2\ell}B$ or $A^{2m-1}B^2$, which has an odd length. The remaining sequence, after excluding $A^{2\ell}B$ or $A^{2m-1}B^2$ from the entire sequence, consists of $(p+q)-1$ blocks each of which is either $A^\ell B$ or A^mB^2. Since the length of the remaining sequence is even, one can see that the number of odd-length blocks in the remaining sequence is even and, consequently, the number of even-length blocks is even as well. Since $\mathcal{F}^{(1)}$ is composed of odd-length blocks and $\mathcal{F}^{(2)}$ pairs of even-length blocks as shown in Eq. (14), the symbol sequence is decomposed into the symbols in $\mathcal{F}^{(1)}$ or $\mathcal{F}^{(2)}$. On the other hand, if $(p+q)$ and t are both even numbers, this is the case of what we have seen in the above argument as for the remaining sequence. Finally, we note that the sequence with an odd $(p+q)+t$ does not appear in $\mathcal{A}$. This is because, as shown in the last paragraph of Appendix B, the periodic orbit of twice repetition of the sequence appears in $\mathcal{A}$. Therefore, $(p+q)+t$ is always even.

The set of periodic orbits $\mathcal{F}$ therefore may play the role of *fundamental cycles* in the hyperbolic systems, and this suggests the application of the *cycle expansion* [33]. Let f_n denote a sum of the linear stability of periodic orbits of period n in $\mathcal{F}$, namely,

$$f_n = \sum_{\{p\in\mathcal{F}|t_p=n\}} \frac{1}{|\Lambda_p|}. \tag{15}$$

In Fig. 6, we compare the behavior of a_n and f_n and find excellent agreement. In particular, as shown in the inset, the difference $|a_n-f_n|$ decreases exponentially. This result strongly suggests that a similar mechanism as the cycle expansion indeed works in the set $\mathcal{A}$, and the contribution from the periodic orbits contained in $\mathcal{A}\backslash\mathcal{F}$ is shadowed by the fundamental periodic orbits $\mathcal{F}$.

We here remark the pruning in the symbolic representation of $\mathcal{A}$. As explained in Appendix B, we have used inequalities (B5) to delimit possible symbol sequences in $\mathcal{A}$. For example, a symbol sequence $A^{\ell_1}BA^{\ell_2}B$ appears only when the conditions $\ell_1<7\ell_2+6$ and $\ell_2<7\ell_1$ are both satisfied. Some subset of periodic orbits is to be pruned by these inequalities, and have actually been pruned in the calculation in Fig. 6. However, at the level of numerical observations, the effect of the pruning is not significant.

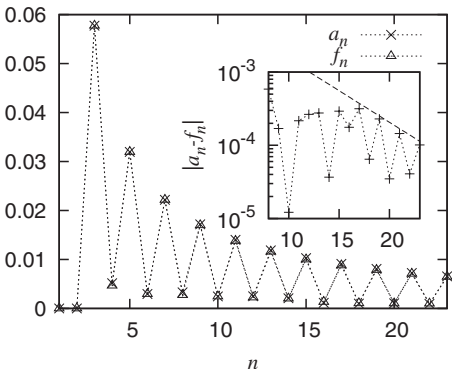

FIG. 6. The crosses and triangles show the coefficients a_n and f_n in the expansion (13). Inset: the difference $|a_n-f_n|$. The broken line is an exponential function fitted to $|a_n-f_n|$ in the large n region.

Survival probability

The result in the previous subsection shows that for large n the coefficients c_n in the whole expansion (12) can be well approximated by the coefficients f_n, the latter plays the role of fundamental cycles in the expansion for the periodic orbits accumulating to FMUPOs. We therefore rewrite the zeta function (8) for our map as

$$\frac{1}{\zeta(z)} \approx 1 - \sum_{p\in\mathcal{F}} \frac{z^{t_p}}{|\Lambda_p|}. \tag{16}$$

In the summation over $\mathcal{F}$, the periodic orbits in $\mathcal{F}^{(1)}$ gives the primary contribution to the expansion (16). The contribution from the set $\mathcal{F}^{(2)}$ in which the stability increases quadratically with respect to the period is roughly estimated as z^k/k^2, and does not affect an analytic property of $1/\zeta$. Thus, it is sufficient to evaluate the periodic orbit expansion (16) only by taking into account the summation over $\mathcal{F}^{(1)}$.

The linear stability for the periodic orbits in $\mathcal{F}^{(1)}$ is given as

$$\Lambda_{A^{2k}B} = 8k+3+\sqrt{(8k+3)^2-1}, \tag{17}$$

$$\Lambda_{A^{2k-1}B^2} = -(48k-7)-\sqrt{(48k-7)^2-1}. \tag{18}$$

For large k the summations over $A^{2k}B$ and $A^{2k-1}B^2$ are, respectively, approximated as

$$\sum_{k=1}^{\infty} \frac{z^{2k+1}}{|\Lambda_{A^{2k}B}|} \approx \frac{1}{2}\sum_{k=1}^{\infty} \frac{z^{2k+1}}{8k+3}, \tag{19}$$

$$\sum_{k=1}^{\infty} \frac{z^{2k+1}}{|\Lambda_{A^{2k-1}B^2}|} \approx \frac{1}{2}\sum_{k=1}^{\infty} \frac{z^{2k+1}}{48k-7}. \tag{20}$$

Now recall a general identity of the series with constants a,b satisfying $|b/a|<1$

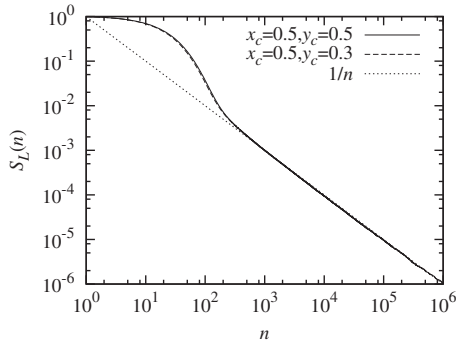

FIG. 7. The survival probability for the map with a leaking region. The leaking region is a square with the side length $\varepsilon=0.2$ centered at (x_c,y_c). The dotted line shows $S_L(n)=n^{-1}$.

$$\sum_{k=1}^{\infty}\frac{z^k}{ak-b}=\frac{1}{a}\sum_{i=1}^{\infty}\left(\frac{b}{a}\right)^{i-1}L_i(z), \tag{21}$$

where

$$L_n(z)=\sum_{k=1}^{\infty}\frac{z^k}{k^n}, \tag{22}$$

is a polylogarithm function, e.g., $L_1(z)=-\log(1-z)$ [34]. This implies that $1/\zeta(z)$ contains logarithmic contributions, $z\log(1-z)$ and $z\log(1+z)$, and we find associated logarithmic branch cuts along $[1,\infty]$ and $[-\infty,-1]$ on the complex z plane. The argument leading to the power law behavior of the survival probability follows that developed in Ref. [25]: the contour of the integration is deformed so as not to cross the branch cuts: the contour for $|z|>1$ is divided into four parts, two half circles in the upper and the lower half plane and two paths along two branch cuts on the real z axis. The dominant contribution to the integration comes from the contours encircling brunch cuts, and the asymptotic behavior of the survival probability is determined by the integral at the branch points. Around $z=1$ for instance, the integrand is expanded as

$$\frac{d}{dz}\log\zeta^{-1}(z)\sim\log(1-z)+\mathcal{O}[(1-z)]. \tag{23}$$

From the general formula $\oint_{\gamma_r}z^{-n}\log(1-z)dz=-2\pi i/n$, the integration along the branch cut $[1,\infty]$ is evaluated by deforming the contour encircling the origin. Applying the same argument for the branch cut $[-\infty,-1]$, we obtain the asymptotic expression of the survival probability as

$$\Gamma_n\sim n^{-1}. \tag{24}$$

In order to confirm that the above argument properly predicts the survival probability $S_L(n)$ of our system, we numerically calculate $S_L(n)$ of the map with a leaking region. The survival probability is defined as Eq. (10), and the initial points are uniformly distributed with equal probability outside the leaking region. We choose the square leaking region centered at (x_c,y_c) taken away from the region in which periodic points of $\mathcal{A}$ are distributed (see Fig. 4). In Fig. 7 the survival probability for two different leaking regions is plotted. As clearly seen, $S_L(n)$ tends to the prediction of the periodic orbit expansions, that is $S_L(n)\sim n^{-1}$.

IV. RECURRENCE TIME DISTRIBUTION

Not a few works have used the recurrence time distribution to capture the nature of the sticky motion in generic Hamiltonian systems [2,8–10,17,20,27,35]. In particular, some of them discussed the universality of the power law exponent.

The definition of the recurrence region seems to be clear, however, in the case of mixed phase space, since inhomogeneity of phase space is an essential ingredient, one needs to choose the position and size $\mu(R)$ of the recurrence region carefully. Usually, the recurrence region R is located at a certain appropriate position where the orbits inside the recurrence region thus chosen are locally hyperbolic. However, if the size $\mu(R)$ is finite and contains a small island, the distribution may suffer uncontrollable effects. In generic mixed systems, it is quite difficult to avoid such a situation no matter how small its size $\mu(R)$ is.

One possible way to avoid the finite size effect of the recurrence region is to define the recurrence time distribution by taking the limit of $\mu(R)\to 0$. This has actually been done in rigorous arguments in a class of one-dimensional hyperbolic map [23,24]. It should be noted that one needs to take the limit carefully even in such a simple setting since nongeneric distribution appears when the center of recurrence region is placed on periodic orbits.

This is a signature of inhomogeneity of phase space, but the situation becomes more subtle if we consider the nonhyperbolic system. This is indeed so even in the present map. As seen in the previous section, FMUPOs are a unique source of stickiness and the system is hyperbolic otherwise. Even if we put the recurrence region in the hyperbolic domain B, it necessarily contains stable manifolds which emanating from periodic orbits accumulating to FMUPOs. The orbits which leave in the close neighborhood of such stable manifolds stay around FMUPOs for a long while and hence contribute to the power law tail of the recurrence time distribution. On the other hand, the orbits close to the stable manifolds of unstable periodic orbits in the hyperbolic domain may return back to the recurrence region without staying around FMUPOs, thus behave as purely hyperbolic orbits. Both types of stable orbits are dense in arbitrary chosen recurrence region.

We illustrate in Fig. 8 how stable manifolds emanating from FMUPOs are running inhomogeneously in a recurrence region. From the construction of periodic orbits accumulating to FMUPOs, we know that these orbits are also exponentially many, which means that both types of stable manifolds occupy the recurrence region with positive Lebesgue measures.

We here examine the validity of the following ansatz in our model. The simplest possible assumption for the recurrence time distribution to satisfy the above argument would be that the distribution is given as a superposition of the exponential distribution, reflecting the hyperbolic nature of the system, and the power law distribution,

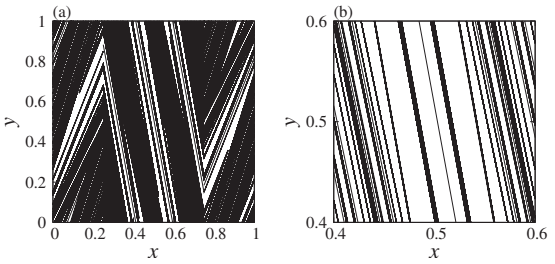

FIG. 8. (a) The stable manifolds of the periodic orbits of $A^{2k}B$, $k=2,3,4,5,6,7$. (b) A magnification of (a) in a square region $0.4<x<0.6$ and $0.4<y<0.6$.

$$P(T) = P_{\text{exp}}(T) + P_{\text{pow}}(T). \tag{25}$$

Now we further assume that the exponent for the power law follows the already reported result, that is $P_{\text{pow}}(T) \sim T^{-3}$ [20]. The exponential part is also supposed to be

$$P_{\text{exp}}(T) \sim \exp[-\mu(R)T]. \tag{26}$$

since the phase space region except for FMUPOs is uniformly hyperbolic [23]. Similar arguments of the superposition of the recurrence time distribution are discussed [16,27].

Our ansatz [Eq. (25)] is simply based on the fact that the orbits with hyperbolic nature dominate the short time scale and the ones controlled by stable manifolds of accumulating periodic orbits contribute to the long-time power law. As is shown in Fig. 9, the distributions clearly exhibit the exponential part in the short time regime and the asymptotic power law part, implying that our proposed form is reasonable. Here, the distribution has been computed using an efficient algorithm with better convergence of the long-time tail, which is presented in Appendix C.

As mentioned above, one possible definition of the recurrence time distribution is given in the limit of $\mu(R) \to 0$, so we next see how the distribution behaves as $\mu(R)$ becomes small. To this end, we pay attention to the normalization of the recurrence time because the average recurrence time

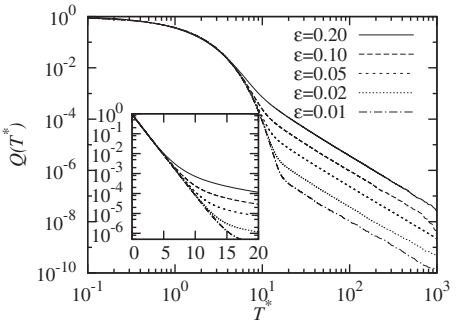

FIG. 9. A plot of the cumulative recurrence time distribution in a log-log scale. The side length of the square recurrence region is denoted by ε. For each distribution, the recurrence time is normalized according to Eq. (27). Inset: the same plot in the log-normal scale. The normalized distribution is an exponential distribution for the short time regime and a power law distribution for the long-time regime. There is a crossover between the two regimes and the crossover time becomes longer as the size of the recurrence region is reduced.

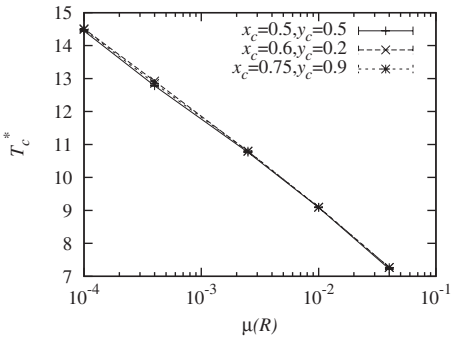

FIG. 10. A plot of the crossover time T_c^* between the exponential and the power law parts of the recurrence time distribution as a function of the area of the recurrence region $\mu(R)$. The cases with different positions are superposed. Each T_c^* is evaluated by fitting the power law part of the distribution.

grows monotonically when the size of recurrence region is reduced. For ergodic systems, it was shown that the average recurrence time is equal to the inverse of $\mu(R)$ [36]. Since our piecewise linear system has ergodicity, we employ the normalized recurrence time

$$T^* = \mu(R)T \tag{27}$$

for different sizes in the recurrence region.

Figure 9 shows that the crossover time between exponential and power law regimes increases as $\mu(R)$ decreases. In these calculations, the recurrence region was chosen as a square with the side length ε. We have checked that the observed trend does not depend on the position and the shape of the recurrence region. We show in Fig. 10 the crossover time T_c^*, which was numerically determined. Clearly, we observe the relation

$$T_c^* \sim -\log[\mu(R)]. \tag{28}$$

This relation implies that T_c^* goes to infinity in the limit of $\mu(R) \to 0$.

The relation of the crossover time is accounted for by the following argument. Let us assume the form of the superposed distribution (25) as

$$P(T) = \begin{cases} C_{\text{exp}} e^{-\mu(R)T} & T < T_p \\ C_{\text{exp}} e^{-\mu(R)T} + C_{\text{pow}} T^{-3} & T \geq T_p \end{cases}, \tag{29}$$

where C_{exp} and C_{pow} are normalization constants. Here we assumed that the power law starts at T_p, for which we only require that T_p should be smaller than the crossover time T_c^*. The normalization condition and the Kac's Lemma concerning the average of the recurrence time [36] is, respectively, expressed as

$$1 = \sum_{T=1}^{\infty} P(T), \tag{30}$$

$$\frac{1}{\mu(R)} = \sum_{T=1}^{\infty} TP(T). \tag{31}$$

The crossover time without normalization $T_c = T_c^*/\mu(R)$ can be determined by solving an implicit relation $C_{\exp}\exp(-\mu(R)T_c) = C_{\mathrm{pow}}T_c^{-3}$, and we get

$$T_c = -\frac{3}{\mu(R)} W\left[-\frac{\mu(R)}{3}\left(\frac{C_{\mathrm{pow}}}{C_{\exp}}\right)^{1/3}\right], \tag{32}$$

where $W(x)$ is the Lambert W function, which is defined as the inverse function of $f(w) = w\exp(w)$ [37]. $W(x)$ is a multiple-valued function in the interval $(-1/e, 0)$. Since $\mu(R)T_c > 1$ meaning that $W(x)$ is smaller than -1, T_c is determined by adopting $W_{-1}(x)$. Now, solving the Eqs. (30) and (31) with respect to $C_{\mathrm{pow}}/C_{\exp}$ with Eq. (29), we have

$$\frac{C_{\mathrm{pow}}}{C_{\exp}} = \frac{\mu(R) - (1 - e^{-\mu(R)})}{\sum_{T=T_p}^{\infty} \frac{1}{T^3} - \mu(R)\sum_{T=T_p}^{\infty} \frac{1}{T^2}} \frac{e^{-\mu(R)}}{(1 - e^{-\mu(R)})^2}. \tag{33}$$

Suppose that $\mu(R)$ is small and that T_p increases more slowly than as $1/\mu(R)$. For sufficiently small $\mu(R)$, T_p can be assumed to be large enough as $\Sigma_{T=T_p}^{\infty} T^{-3} \sim T_p^{-2}$. It leads

$$\frac{C_{\mathrm{pow}}}{C_{\exp}} \sim T_p^2 + \mathcal{O}[\mu(R)], \tag{34}$$

and then $\mu(R)(C_{\mathrm{pow}}/C_{\exp})^{1/3}/3$ is small. For a small positive x, we have $W_{-1}(-x) \sim \log(x)$. Therefore we reach our expected relation for the crossover time,

$$T_c^* = \mu(R)T_c \sim -\log[\mu(R)]. \tag{35}$$

The arguments on the crossover time are self-consistent, which is another evidence for the validity of our ansatz [Eq. (25)].

The result shows that as long as we adopt the normalization [Eq. (27)] for the recurrence time, which is certainly one plausible choice, one has to conclude that the recurrence time distribution tends to obey an exponential function as the size of the recurrence region goes to zero. The reason why the crossover time T_c^* grows to infinity is that the stickiness around FMUPOs significantly prolongs the average recurrence time. However, the FMUPOs does not affect the average recurrence time $1/\mu(R)$ since FMUPOs have null measure in phase space. The situation must be much complex in generic mixed systems with hierarchical invariant structures. These observations suggest the subtleness in claiming the universality of the recurrence time distribution in the system with sticky regions on a mathematically rigorous ground.

V. CONCLUSIONS AND DISCUSSIONS

We have investigated the stickiness of a two-dimensional piecewise linear map which has a family of marginal unstable periodic orbits (FMUPOs) in phase space. Since the phase space of generic Hamiltonian systems is complicated, it is reasonable to study the simplest possible systems. Although some generic features might be lost in the simplification, which is certainly the price we have to pay, it would be an inevitable step to have a better understanding of the issue. The piecewise linear map we have studied here has simple phase space structures exactly because of piecewise linearity of each region. However, for generic K the boundary between regular and chaotic components is still difficult to describe [7,28], thus we have focused on the case with specific values of K, for which there is a proof showing that the boundary between regular and chaotic components is composed of strictly straight lines [28]. Since regular components in phase space for such specific values of K are composed of periodic orbits with fixed period, not irrational rotations on ordinary KAM curves, the obtained result may reflect specific natures of the system. Here we have further limited ourselves to the case $K=4$ in which only FMUPOs lie as nonhyperbolic components.

We first showed that there exists a series of unstable periodic orbits which accumulate to FMUPOs. (The result is generalizable to the case with the sharply divided phase space for $K_n = 2(1+\cos\frac{\pi}{n})$ $(n=2,3,\ldots)$.) Each periodic orbit is labeled by a sequence of two symbols, and the observation for this symbolic coding reveals that stabilities of these periodic orbits increase as a polynomial function of its period. Note that unstable periodic orbits with a similar property have been found for other systems as the stadium and Sinai billiards and also for the systems with sharply divided phase space [6,30].

In addition, we could specify the region in which accumulating periodic orbits exist, which means that the "sticky zone" is only a part of phase space, not gradually extended to the entire phase space. This fact enables us to design the system for which the survival probability from the FMUPOs is examined. If choosing the leaking region such that it lies outside the sticky zone, we can realize an open system with all the accumulating periodic orbits being untouched.

For such an open system, we have applied the periodic orbit theory, especially evaluated the survival probability via the dynamical zeta function. Since the periodic orbit expansion requires all the periodic orbits of the system, it is not easy in general to apply to the system without a good symbolic dynamics associated with generating partitions. However, thanks to the piecewise linearity and the existence of an efficient symbolic coding, though it is not generating, we could enumerate all the periodic orbits numerically. More importantly we have revealed that the cancellation mechanism works in the set of accumulating periodic orbits. That is, among accumulating periodic orbits with polynomial stability, the periodic orbits with linearly increasing stability, the slowest growth rate, play the role of fundamental cycles in the periodic orbit expansion, and the contribution from the rest of accumulating orbits with faster growth rate, but still polynomial, is cancelled by the fundamental cycles. The situation is quite similar to the hyperbolic system where the cycle expansion works using the shadowing mechanism between periodic orbits [33]. Assuming the dynamical zeta function only including the periodic orbits with linearly increasing stability, we have derived the power law decay of the survival probability, which shows good agreement with the numerically obtained survival probability.

In the second part, we have analyzed the recurrence time distribution, which is often used to discuss the slow motion.

For the survival probability, we have only to concentrate on the slowest rate-controlling process and we can forget about escaping orbits. The recurrence time distribution is a similar measure as the survival probability, but it more reflects global nature of the phase space.

We here discussed some ambiguities in its definition, that is, the position or size of the recurrence region R. Our numerical observation shows that the recurrence time distribution has the exponential part in a short time regime and the asymptotic power law part. It also shows that there is a crossover time T_c^* between the two regimes, and T_c^* varies depending on the size of the recurrence region. Assuming that the recurrence time distribution is a superposition of the exponential distribution and the power law distribution, we derive the behavior as $T_c^* \sim -\log[\mu(R)]$, which has been confirmed numerically. This implies that as the size of the recurrence region $\mu(R)$ gets smaller the exponential part tends to dominate the recurrence time distribution. Therefore, when adopting a canonical definition for the recurrence region, as is introduced in one-dimensional maps [23], one must conclude that the recurrence time distribution is exponential, and the power law decay usually claimed in the literature is regarded as a finite size effect.

ACKNOWLEDGMENTS

One of authors (A.A.) would like to thank M. Hirata and P. Cvitanović for useful discussions. This work is supported by Grants-in-Aid for Scientific Research (C) No. 18540378 for the Ministry of Education, Culture, Sports, Science and Technology of Japan.

APPENDIX A: A PROCEDURE TO ENUMERATE PERIODIC ORBITS

Assuming that the map is composed of ℓ distinct piecewise linear regions in general, we here give a method to compute the periodic orbits. We consider the case of two-dimensional maps while the generalization to higher-dimensional maps is easily implementable. Let $\{s_n\}_{n=1}^{\ell}$ be the symbols assigned to each piecewise linear region, then we expressed the map as

$$\begin{pmatrix} x' \\ y' \end{pmatrix} \equiv M_{s_n} \begin{pmatrix} x \\ y \end{pmatrix} + C_{s_n} \quad \text{if } (x,y) \in s_n \mod 1, \tag{A1}$$

where M_{s_n} is a constant real matrix which satisfies $\det M_{s_n} = 1$ and C_{s_n} a constant real vector. We assign symbols s_n to each orbit according to which region the orbit visits. Then periodic orbits are represented as the repetition of a finite sequence. We consider a periodic orbit with period p whose corresponding symbol is given by $S_1 S_2 \cdots S_p$ where $S_i \in \{s_1, s_2, \ldots, s_\ell\}$. The condition for the periodicity is expresses as

$$M_{S_1} \begin{pmatrix} x_1 \\ y_1 \end{pmatrix} + C_{S_1} \equiv \begin{pmatrix} x_2 \\ y_2 \end{pmatrix} \mod 1,$$

$$M_{S_2} \begin{pmatrix} x_2 \\ y_2 \end{pmatrix} + C_{S_2} \equiv \begin{pmatrix} x_3 \\ y_3 \end{pmatrix} \mod 1,$$

$$\vdots$$

$$M_{S_p} \begin{pmatrix} x_p \\ y_p \end{pmatrix} + C_{S_p} \equiv \begin{pmatrix} x_1 \\ y_1 \end{pmatrix} \mod 1, \tag{A2}$$

where (x_i, y_i) is the ith periodic point contained in the region S_i. This can be rewritten as

$$M_{(1)} \begin{pmatrix} x_1 \\ y_1 \end{pmatrix} - \begin{pmatrix} x_2 \\ y_2 \end{pmatrix} = \begin{pmatrix} n_1 \\ m_1 \end{pmatrix} - C_{(1)},$$

$$M_{(2)} \begin{pmatrix} x_2 \\ y_2 \end{pmatrix} - \begin{pmatrix} x_3 \\ y_3 \end{pmatrix} = \begin{pmatrix} n_2 \\ m_2 \end{pmatrix} - C_{(2)},$$

$$\vdots$$

$$M_{(p)} \begin{pmatrix} x_p \\ y_p \end{pmatrix} - \begin{pmatrix} x_1 \\ y_1 \end{pmatrix} = \begin{pmatrix} n_p \\ m_p \end{pmatrix} - C_{(p)}, \tag{A3}$$

where (n_i, m_i) is a pair of integers determined from the left-hand side of the ith equation in Eq. (A2). Note that the maximal and minimal values of n_i and m_i are finite. By solving these equations with respect to (x_i, y_i) $(i=1,2,\ldots)$, we obtain

$$\begin{aligned} \begin{pmatrix} x_1 \\ y_1 \end{pmatrix} = (M_p M_{p-1} \cdots M_1 - I)^{-1} \Bigg\{ & M_p M_{p-1} \cdots M_2 \left(\begin{pmatrix} n_1 \\ m_1 \end{pmatrix} - C_{(1)} \right) \\ & + M_p M_{p-1} \cdots M_3 \left(\begin{pmatrix} n_2 \\ m_2 \end{pmatrix} - C_{(2)} \right) \\ & + \cdots + \left(\begin{pmatrix} n_p \\ m_p \end{pmatrix} - C_{(p)} \right) \Bigg\}, \end{aligned}$$

$$\begin{aligned} \begin{pmatrix} x_2 \\ y_2 \end{pmatrix} = (M_1 M_p \cdots M_2 - I)^{-1} \Bigg\{ & M_1 M_p \cdots M_3 \left(\begin{pmatrix} n_2 \\ m_2 \end{pmatrix} - C_{(2)} \right) \\ & + M_1 M_p \cdots M_4 \left(\begin{pmatrix} n_3 \\ m_3 \end{pmatrix} - C_{(3)} \right) \\ & + \cdots + \left(\begin{pmatrix} n_1 \\ m_1 \end{pmatrix} - C_{(1)} \right) \Bigg\}, \end{aligned}$$

$$\vdots$$

$$\begin{aligned} \begin{pmatrix} x_p \\ y_p \end{pmatrix} = (M_{p-1} \cdots M_1 M_p - I)^{-1} \Bigg\{ & M_{p-1} \cdots M_1 \left(\begin{pmatrix} n_p \\ m_p \end{pmatrix} - C_{(p)} \right) \\ & + M_{p-1} \cdots M_2 \left(\begin{pmatrix} n_1 \\ m_1 \end{pmatrix} - C_{(1)} \right) \\ & + \cdots + \left(\begin{pmatrix} n_{p-1} \\ m_{p-1} \end{pmatrix} - C_{(p-1)} \right) \Bigg\}. \end{aligned} \tag{A4}$$

We then substitute possible values of integers $\{n_i, m_i\}_{i=1}^{p}$ into the right-hand side of Eq. (A4), and check whether or not the resulting (x_i, y_i) is consistent with the conditions $(x_i, y_i) \in S_i$ $(i=1,2,\ldots,k)$. If (x_i, y_i) is in the region S_i for all i, the desired periodic orbit is obtained.

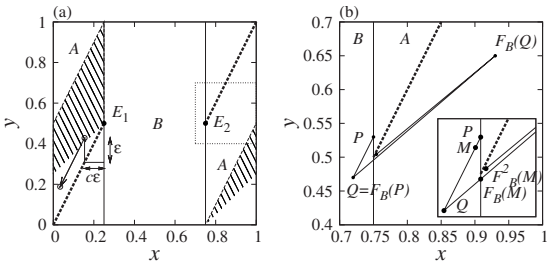

FIG. 11. (a) FMUPOs and the point moving along FMUPOs. The region $\mathcal{I}$ is shown in a shaded area, and the broken line represents FMUPOs. The point inside $\mathcal{I}$ shown as an open circle moves parallel to FMUPOs. $c\epsilon$ and ϵ represent the distance from FMUPOs in the x and y directions, respectively. (b) The plot of the time evolution by F_B around the end point of FMUPOs E_2 (the square region enclosed by dotted lines in (a)), and the inset is its magnification. The points P,M,Q represent (x_1,y_1) for $d=0$, $d=1/7$ and $d=1$, respectively. The time evolution of line segments is shown ignoring the symmetry of the map: the line segment $\overline{PM}$ moves to $F_B(Q)F_B^2(M)$ the line segment $\overline{MQ}$ moves to $F_B(M)F_B(Q)$. $F_B(M)$ lies on $x=3/4$.

APPENDIX B: UNSTABLE PERIODIC ORBITS ACCUMULATING TO FMUPOS

In this appendix, we show the existence of a series of unstable periodic orbits close to FMUPO in the map [Eq. (5)]. To this end, let us first consider the region parametrized by the variables (c,ϵ)

$$\mathcal{I} := \{(x,y) = (1/4 - c\epsilon, 1/2 + \epsilon - 2c\epsilon) | 0 < \epsilon \leq 1/2 \text{ and } 0 \leq c < 1\}. \tag{B1}$$

Here the point $E_1=(1/4,1/2)$ is one of the end points of FMUPOs and the region $\mathcal{I}$ is shown as a shaded area in Fig. 11(a).

It is easy to check that the orbit leaving $\mathcal{I}$, $F^i(x_0,y_0)$ $((x_0,y_0)\in\mathcal{I})$, moves parallel to FMUPOs for $0\leq i<n$, where n is given as

$$n = \left[\frac{1}{2\epsilon} - c\right] + 1. \tag{B2}$$

Here $[x]$ denotes the integer part of x. After n steps, the point enters the region B.

Next we denote the map [Eq. (5)] in the region A and B by F_A and F_B, respectively, and define the symmetric transformation with respect to the center of phase space as $S(x,y) := (1-x,1-y)$. Suppose that the point $(x_0,y_0)\in\mathcal{I}$ is mapped to (x_1,y_1) up to the symmetry, that is, $F_A^n(x_0,y_0) = S^n(x_1,y_1)$. Here we express (x_1,y_1) using an alternative set of parameters (d,ϵ) as $(x_1,y_1)=(3/4-d\epsilon,1/2+\epsilon-2d\epsilon)$, where

$$d = n - \left(\frac{1}{2\epsilon} - c\right). \tag{B3}$$

The time evolution of (x_1,y_1) by F_B, near the opposite end point $E_2=(3/4,1/2)$, differs depending on d, as shown in Fig. 11(b). For $1/7\leq d<1$, the point (x_1,y_1) enters A in a single iteration, and we have $F_B(x_1,y_1)=S(3/4-\epsilon+7d\epsilon,1/2-\epsilon+6d\epsilon)$. For $0\leq d<1/7$, (x_1,y_1) stays B in a single iteration and enters A in the next iteration. Then we have $F_B^2(x_1,y_1) = S^2(3/4+6\epsilon-41d\epsilon,1/2+5\epsilon-34d\epsilon)$. In Fig. 11(b) we depict the evolution of (x_1,y_1) by line segments (see the caption).

In this way, the point (x_1,y_1) comes back, up to the symmetry with respect to S, to the initial region $\mathcal{I}$. Therefore we can construct the map on $\mathcal{I}$ as

$$F(x_0,y_0) = \begin{cases} F_1 := F_B \circ F_A^n(x_0,y_0) & \frac{1}{7} \leq d < 1 \\ F_2 := F_B^2 \circ F_A^n(x_0,y_0) & 0 \leq d < \frac{1}{7} \end{cases}. \tag{B4}$$

In order to obtain periodic orbits, it suffices to solve the equation $F^s(x_0,y_0)=(x_0,y_0)$ for $s=1,2,\ldots$. The simplest one is to solve the equation $F(x_0,y_0)=(x_0,y_0)$. In this case, we solve the equations $F_1(x_0,y_0)=(x_0,y_0)$ and $F_2(x_0,y_0)=(x_0,y_0)$ for given n, taking into account the symmetry: in the first equation in Eq. (B4), n has to be an odd integer. Similarly, n has to be an even integer for F_1, then we have periodic orbits in the forms of $F_B\circ F_A^{2k}$ and $F_B^2\circ F_A^{2k-1}$ $(k=1,2,\ldots)$ (Fig. 12). On the other hand, in the case of odd n for F_1, the twice repetition of F_1, i.e., $F_B\circ F_A^{2k-1}\circ F_B \circ F_A^{2k-1}$ turns out to be periodic orbits, and similarly in the case of even n for F_2, the twice repetition of F_2, i.e., $F_B^2 \circ F_A^{2k}\circ F_B^2\circ F_A^{2k}$ gives periodic orbits.

Also for $s\geq 2$, the set of equations has solutions at least formally since we have $2s$ equations for $2s$ variables (x_j,y_j) $(j=1,2,\ldots,s)$. Here (ϵ_j,c_j) represent the set of parameters for each (x_j,y_j). However, for $s\geq 2$, not all of solution are not necessarily the periodic orbits. To show this, for each (ϵ_j,c_j), we put n_j as the sequence of integers determined $n_j=[1/2\epsilon_j-c_j]+1$, and also $d_j=c_j+n_j-1/2\epsilon_j$. Since there exists a mapping relation (B4), we necessarily have some relation between successive n_i and n_{i+1}. More explicitly, they are expressed as

$$n_{i+1} \leq 7n_i + 6, \quad n_i \leq 7n_{i+1} \quad \frac{1}{7} \leq d_i < 1,$$

$$n_{i+1} \leq 7n_i + 5, \quad n_i \leq 7n_{i+1} - 1 \quad 0 \leq d_i < \frac{1}{7}. \tag{B5}$$

Due to these conditions, for some given sequence $(n_1,n_2,\ldots,n_s)$, the formal solution for $F^s(x_0,y_0)=(x_0,y_0)$ cannot be the periodic orbit. This means that the *pruning* of the periodic orbits happens for $s\geq 2$.

In addition, similarly in the case of $s=1$, the symmetry must be taken into account. The formal solution is periodic if $N=s+\Sigma_{j=1}^s n_j+i_j$ is an even number, where $i_j=1$ for F_1 and $i_j=2$ for F_2. For odd N, the twice repetition leads periodic orbits.

APPENDIX C: AN EFFICIENT ALGORITHM TO CALCULATE THE RECURRENCE TIME DISTRIBUTION IN ERGODIC SYSTEMS

The ordinary algorithm to calculate the recurrence time distribution requires a uniform ensemble of initial points in

the recurrence region. We here introduce an alternative algorithm for practical computations using a uniform ensemble in phase space.

Let X be phase space and f be a differentiable function onto X and μ be an invariant measure, that is $\forall A \subset X$, $\mu(A)=\mu[f^{-1}(A)]$. Let us assume that a dynamical system (X,f,μ) is ergodic. Due to the ergodicity, for $\forall x_0 \in X$, the measure of a compact region $R \subset X$ can be given by the time average,

$$\mu(R) = \lim_{T\to\infty} \frac{1}{2T} \sum_{i=-T}^{T-1} \mathbf{1}_R[f^i(x_0)], \tag{C1}$$

where $\mathbf{1}_R(x)$ is the indicator function of R, i.e., $\mathbf{1}_R(x)=1$ if $x \in R, 0$ if $x \notin R$. Let us consider a segment of the trajectory $\{f^s(x),\ldots,f^{s+t}(x)\}$ which starts from R and returns to R, $f^s(x)$, $f^{s+t}(x) \in R$ and $f^i(x) \notin R (s<i<s+t)$. The recurrence time of the segment is t. A single segment of the recurrence time t makes a contribution of $t-1$ points of the trajectory in the region outside R (Fig. 12). The points of the recurrence segment in $X \backslash R$ have the weight,

$$w_t = \frac{1}{t-1}. \tag{C2}$$

Since for the weight [Eq. (C2)] the recurrence time has to be $t \geq 2$, the recurrence segments for $t=1$ are not taken account in $X \backslash R$. The algorithm to calculate the recurrence time distribution using a uniform ensemble in phase space is given as follows:

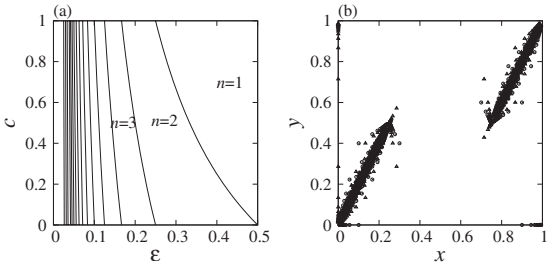

FIG. 12. (a) The partition of (ϵ,c) space divided with different values of n providing the relation (B2). (b) Plot of periodic points of $F_A^{2k} \circ F_B$ (circle) and $F_A^{2k-1} \circ F_B^2$ (triangle) for $k=1,2,\ldots,20$.

(1) Choose an initial point $x \in X$ from a uniform ensemble in phase space.

(2) In case of $x \notin R$, calculate the recurrence time t by the forward and backward iteration, and put the corresponding weight as $w_t=1/(t-1)$.

(2′) In case of $x \in R$, check $f(x) \in R$ or not. If $f(x) \in R$, put the weight as $w_{t=1}=1$. Otherwise, discard x.

(3) Evaluate the distribution of the recurrence time with the weight w_t from the ensemble.

Note that the procedure (2′) gives the probability for the recurrence time $t=1$.

The algorithm we introduced here is efficient in convergence of the tail of the distribution. Since the weight w_t decreases as t increases, the longer recurrent segments in the computation are detectable from the ensemble comparing to the ordinary algorithm.

[1] C. F. F. Karney, Physica D **8**, 360 (1983).
[2] B. V. Chirikov and D. L. Shepelyansky, Physica D **13**, 395 (1984).
[3] J. D. Meiss, Rev. Mod. Phys. **64**, 795 (1992).
[4] R. Mackay, J. Meiss, and I. Percival, Physica D **13**, 55 (1984).
[5] J. D. Meiss and E. Ott, Phys. Rev. Lett. **55**, 2741 (1985).
[6] K.-C. Lee, Physica D **35**, 186 (1989).
[7] J. Malovrh and T. Prosen, J. Phys. A **35**, 2483 (2002).
[8] H. Tanaka and A. Shudo, Phys. Rev. E **74**, 036211 (2006).
[9] G. Cristadoro and R. Ketzmerick, Phys. Rev. Lett. **100**, 184101 (2008).
[10] R. Venegeroles, Phys. Rev. Lett. **102**, 064101 (2009).
[11] E. G. Altmann and T. Tél, Phys. Rev. Lett. **100**, 174101 (2008).
[12] E. G. Altmann and T. Tél, Phys. Rev. E **79**, 016204 (2009).
[13] V. Afraimovich and G. M. Zaslavsky, Phys. Rev. E **55**, 5418 (1997).
[14] Y. Aizawa, Prog. Theor. Phys. **81**, 249 (1989).
[15] B. V. Chirikov and D. L. Shepelyansky, Phys. Rev. Lett. **82**, 528 (1999).
[16] N. Buric, A. Rampioni, G. Turchetti, and S. Vaienti, J. Phys. A **36**, L209 (2003).
[17] M. Weiss, L. Hufnagel, and R. Ketzmerick, Phys. Rev. Lett. **89**, 239401 (2002).
[18] M. Weiss, L. Hufnagel, and R. Ketzmerick, Phys. Rev. E **67**, 046209 (2003).
[19] E. G. Altmann, A. E. Motter, and H. Kantz, Chaos **15**, 033105 (2005).
[20] E. G. Altmann, A. E. Motter, and H. Kantz, Phys. Rev. E **73**, 026207 (2006).
[21] T. Miyaguchi, Phys. Rev. E **75**, 066215 (2007).
[22] D. N. Armstead, B. R. Hunt, and E. Ott, Physica D **193**, 96 (2004).
[23] M. Hirata, Ergod. Theory Dyn. Syst. **13**, 533 (1993).
[24] M. Hirata, B. Saussol, and S. Vaienti, Commun. Math. Phys. **206**, 33 (1999).
[25] R. Artuso, P. Cvitanović, and G. Tanner, Prog. Theor. Phys. **150**, 1 (2003).
[26] B. V. Chirikov, e-print arXiv:nlin/0006013.
[27] H. Hu, A. Rampioni, L. Rossi, G. Turchetti, and S. Vaienti, Chaos **14**, 160 (2004).
[28] M. Wojtkowski, Commun. Math. Phys. **80**, 453 (1981).
[29] A. Akaishi and A. Shudo, in *Let's Face Chaos through Nonlinear Dynamics*, Proceedings of Let's Face Chaos through Nonlinear Dynamics 7th International Summer School and Conference, edited by M. Robnik and V. Romanovski (AIP, New York, 2008), Vol. 1076, pp. 1–4.
[30] G. Tanner, J. Phys. A **30**, 2863 (1997).
[31] P. Gaspard, *Chaos, Scattering and Statistical Mechanics* (Cambridge University Press, Cambridge, England, 1998).

[32] P. Cvitanović, R. Artuso, R. Mainieri, G. Tanner, and G. Vattay, *Chaos: Classical and Quantum* (Niels Bohr Institute, Copenhagen, 2008).
[33] R. Artuso, E. Aurell, and P. Cvitanovic, Nonlinearity **3**, 325 (1990).
[34] L. Lewin, *Polylogarithms and Associated Functions* (North-Holland, New York, 1981).
[35] N. Hadyn, J. Luevano, G. Mantica, and S. Vaienti, Phys. Rev. Lett. **88**, 224502 (2002).
[36] M. Kac, Bull. Am. Math. Soc. **53**, 1002 (1947).
[37] R. M. Corless, G. H. Gonnet, D. E. G. Hare, D. J. Jeffrey, and D. E. Knuth, Adv. Comput. Math. **5**, 329 (1996).